# Observations of the Response of Sea Waves to Veering Winds

DIANE MASSON

*Institute of Ocean Sciences, Sidney, BC, Canada*

(Manuscript received 19 March 1990, in final form 4 June 1990)

ABSTRACT

A data-adaptive technique, the iterative maximum likelihood method, is used to estimate directional wave spectra from data collected by three pitch-and-roll buoys, during two turning wind events of the CASP 86 experiment. A relaxation coefficient is estimated for the response of both the mean wave direction for each frequency band and the main wave direction of the wind sea spectrum to a change in wind direction. The values of the coefficients are found to be consistent with each other, and within the scatter of previous estimates. Also, a definite correlation is established between the wave rms angular spread and the rate of change of wind direction. Finally, the shapes of the estimated directional distributions are tested for symmetry and unimodality. A significant proportion of the estimated distributions are found to be neither unimodal nor symmetric.

## 1. Introduction

A description of the wind-generated surface gravity wave field, including its directional characteristics, provides valuable information for many engineering and scientific applications. The directional frequency power spectrum, $F(f, \theta)$, which gives the distribution of wave energy at different frequency, $f$, and direction of propagation, $\theta$, is commonly represented as the product of a frequency spectrum, $E(f)$, and a directional spreading function, $D(f, \theta)$:

$$F(f, \theta) = E(f)D(f, \theta), \tag{1}$$

where

$$\int_{-\pi}^{\pi} D(f, \theta)d\theta = 1.$$

The exact shape of the directional distribution is determined by the combined action of the energy input from the atmosphere, the dissipation mostly due to wave breaking, and the nonlinear interactions among spectral components. In the case of a homogeneous stationary wind field, the angular distribution of ocean wave energy has been extensively documented (e.g., Mitsuyasu et al. 1975; Donelan et al. 1985). Different parameterizations have been proposed to model the observed spreading function in which the distribution is centered around the wind direction and narrower near the peak frequency (the frequency where the energy is maximum).

Although more complex wind fields, such as a rapidly changing wind direction, are often encountered in nature, information on the associated wind seas is scarce. Field observations of the response of the mean wave direction of individual frequency bands to veering winds has been presented by Hasselmann et al. (1980), and Allender et al. (1983). In the former, a simple model was introduced to describe the observed wave directional relaxation:

$$\frac{\partial \bar{\theta}(f)}{\partial t} = B\omega \sin(\theta_w - \bar{\theta}(f)) \tag{2}$$

where $\bar{\theta}(f)$ is the estimated mean direction for a spectral band centered around frequency $f$, $\theta_w$ is the wind direction, and $\omega = 2\pi f$ is the angular frequency. From a one parameter regression analysis, they obtained an average relaxation coefficient $B = 2.0 \times 10^{-5}$. Allender et al. (1983) extended the above relationship to include a wind speed dependency by including the extra factor $U/c(f)$ in (2), with $U$ the wind speed at a 10 m height, and $c(f)$ the wave phase speed. In both studies, the measured directional relaxation time, $(B\omega)^{-1}$, decreases with frequency as the high frequency bands align more quickly to the changing wind direction. The directional relaxation coefficients, $B$, estimated in these two earlier studies, although they present a large scatter, are similar, and without any clear dependency on the wind speed. Hasselmann et al. (1980) also tried to relate the rms angular deviation of energy from the mean direction to the wind forcing but they were unable to establish a definite correlation consistent through the whole dataset.

A different approach to the problem of directional relaxation which may be more suitable to parametric wave hindcast models has been adopted by Günther et al. (1981) and Holthuijsen et al. (1987). They analyzed the response of one main wave direction, av-

*Corresponding author address:* Dr. Diane Masson, Institute of Ocean Sciences, Sidney, BC, Canada, V8L 4B2.

eraged over all wind sea frequencies, to a turning wind. From very limited datasets, their estimates of the relaxation time scale for this main wave direction also display a large scatter and are significantly larger than the equivalent ones derived from the results of the two aforementioned studies. Finally, Young et al. (1987) investigated the role of the complex wave–wave nonlinear interactions in the wave response to a sudden change in wind direction through numerical experimentation with two wave models that compute, or nearly approximate, the exact nonlinear source term. Their results are in qualitative agreement with the ones previously cited, with the high frequency components responding more quickly to a wind shift than the low frequency components. However, the relaxation time scale associated with their model output is a function of wind speed as well as frequency, and has a value between the estimates of the first and second approach mentioned above. Also, their results show a marked difference in the directional response for small and large changes in wind direction. For small wind shifts, the spectrum gradually rotates to the new wind direction, while for large wind shifts a second independent wave system develops in the new wind direction, with the old system gradually decaying. These numerical results were later confirmed by van Vledder and Holthuijsen (1988) who repeated the experiments of Young et al. (1987). Their study also included a small set of observations for which the relaxation time scale of the main wave direction is in the range of the similar time scale estimates reported in the aforementioned studies.

The objective of this study is to complement the rather scarce existing data on the nature of the directional wave spectrum generated by a turning wind. Data collected during the Canadian Atlantic Storm Project (CASP) 1986 by three (Wavec) directional wave buoys are analyzed for two turning wind events. In order to obtain the highest possible directional resolution from the pitch-and-roll buoys, the iterative maximum likelihood method is used to compute the spreading function. From the estimated directional spectra, the response of both the mean direction for each frequency band and the main wave direction for the whole sea spectrum are analyzed, and the relaxation time scales compared with the results of the various studies mentioned above. Also, a definite correlation is established for the first time between the directional spread and the change in wind direction. Finally, the shape of the estimated directional distributions is tested for unimodality and symmetry.

## 2. Data retrieval and analysis

The measurements discussed here were made in conjunction with CASP, offshore from Martinique Beach, Nova Scotia, in February 1986. The three Datawell Wavec (pitch-and-roll) buoys were deployed on a 30 km line running offshore on a bearing of 340°–160° (T), in water depths of 22 (WC 31), 50 (WC 32), and 100 (WC 33) m (Fig. 1). The buoys were recording for 30 min periods on every hour, at a sampling rate of 0.78125 s. The wind vector was measured at the beach by a 10 m mesonet tower, and at the seaward end of the wave array by a Coastal Climate Minimet buoy at a 3 m height. The Minimet winds were converted to the 10 m standard height taking the atmospheric stability into account. In this study, the 10 m wind speed and direction were obtained from the mean of the hourly averaged vector winds derived from wind data recorded at these two stations. In Dobson et al. (1989), the wave component of the CASP 86 experiment is discussed in greater detail, as well as an extensive analysis of the fetch limited growth curves of the measured frequency spectra.

From the time series of the vertical acceleration and the north and east components of the slope recorded by the pitch-and-roll buoys, a cross-spectral matrix was estimated with a resolution of 0.005 Hz and 18 degrees of freedom. To attain statistically reliable estimates, the sample spectra were smoothed by averaging over three adjacent frequency bands, giving spectral estimates with bandwidth 0.015 Hz and 54 degrees of freedom. Also, in the correlation analysis presented below, the mean wave direction and the rms directional spread derived from the smoothed spectra were averaged over two adjacent frequency bands to reduce the amount of data presented.

In general, the directional spectra derived from a pitch-and-roll buoy are of relatively low resolution primarily because it only measures three variables, but also because the conventional data processing techniques do not use the full potential of the data. A standard procedure used to extract the spreading function, $D(f, \theta)$, from the limited amount of information recorded by the directional buoy is to estimate the function with a truncated Fourier series whose first five coefficients are obtained from the cross-spectral data matrix (Longuet-Higgins et al. 1963). To avoid negative spectral values, the directional distribution may be convolved with an arbitrary weighting function, at the expense of a loss of resolution. Another frequently used method is to fit the data to a function of the form $\cos^{2s}[(\theta - \bar{\theta})/2]$, with $\bar{\theta}$ the average direction. The obvious shortcoming of this method is that only unidirectional distributions are properly estimated. Also, Kuik et al. (1988) proposed a simple and computationally efficient method to extract from the Fourier coefficients directional model-free parameters that provide some directional spectral information that may be sufficient in many routine applications.

Because of the complicated forms of the directional wave spectra expected in turning winds, and also because the present objective is not to attain computational efficiency but to obtain the highest possible directional resolution, a higher performance method was applied in this study, the maximum likelihood method

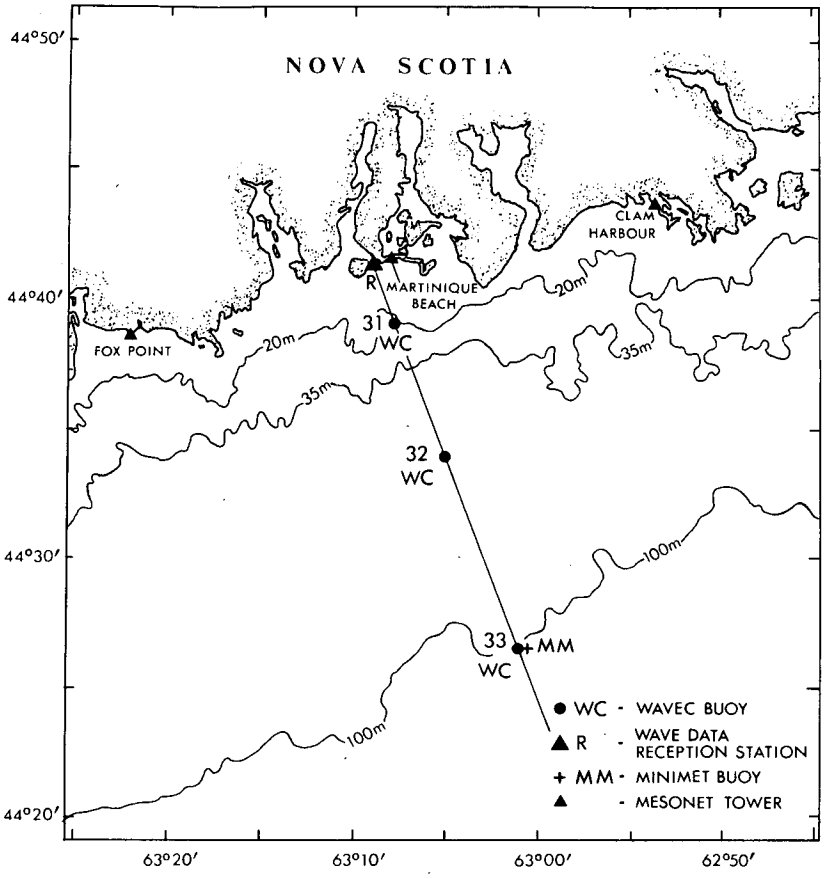


FIG. 1. The CASP directional wave buoy array.

(MLM). This data adaptive directional spectrum estimator has been proved to achieve improved resolution without any a priori assumptions about the spectral shape (e.g., Oltman-Shay and Guza 1984). The methodology is based on the minimization of the estimate variance subject to the constraint that the amplitude of a pure plane wave is passed with unit gain. The MLM estimate of the wave spectrum from a pitch-and-roll buoy takes the form

$$\hat{F}(f, \theta) = \frac{A}{\boldsymbol{\beta}' \mathbf{C}^{-1} \boldsymbol{\beta}} \tag{3}$$

where $\mathbf{C}^{-1}$ is the inverse of the measured cross-spectral data matrix, $\mathbf{C}$. The vector $\boldsymbol{\beta}'$ is the conjugate transpose of the column vector $\boldsymbol{\beta}$ for which the components are 1, $ik\cos\theta$, and $ik\sin\theta$ (with $k$ the wavenumber). The normalization factor $A$ is required to obtain the correct integrated energy density, $\int_0^{2\pi} \hat{F}(f, \theta) d\theta = E(f)$. In evaluating (3), the wavenumber $k$ was derived from the measured cross-spectral matrix rather than from the frequency (through the linear wave dispersion relation) to avoid possible errors caused by unequal sensor calibrations or by unreliable water depth and current information.

Although it performs generally better than non data-adaptive methods, the MLM is not consistent with the data; the cross-spectral matrix constructed from the spectral estimate will in most cases be different from the original cross-spectral data matrix. Pawka (1983) proposed a modified method, the iterative maximum likelihood method (IMLM), in which iterative modifications are made to the MLM estimate to make it more consistent with the data. The IMLM algorithm used here can be written as

$$\hat{F}_{n+1} = \hat{F}_n(f, \theta)\left(1 + \frac{1}{\gamma}\frac{|\lambda|^{\alpha+1}}{\lambda}\right), \tag{4}$$

where $\hat{F}_n(f, \theta)$ is the $n$th iterative modified estimate, $\alpha$ and $\gamma$ are variable parameters that dictate the convergence rate of the algorithm, and

$$\lambda = 1 - \frac{T_n(f, \theta)}{\hat{F}_0(f, \theta)}, \tag{5}$$

with $\hat{F}_0(f, \theta)$ the original MLM spectral estimate, and $T_n(f, \theta)$ the MLM estimate derived from the cross-spectral matrix reconstructed from $\hat{F}_n(f, \theta)$. With increasing iterations, $T_n(f, \theta)$ approaches the initial estimate $\hat{F}_0(f, \theta)$. A series of tests were performed on

different synthetic spectra in order to determine the optimal values of the two convergence parameters. Values of $\alpha = 1$ and $\gamma = 4$ were found to be a good compromise between rapidity of convergence and accuracy of the final estimate. For application of the iterative algorithm on real data, a convergence criteria was chosen, following Krogstad et al. (1988), as

$$\frac{|T_n(f,\theta) - \hat{F}_0(f,\theta)|_{\max}}{E(f)} \leq 0.01. \qquad (6)$$

In most cases, the chosen values of the convergence parameters lead to convergence, according to (6), in less than 30 iterations.

## 3. Results and discussion

From the three month period over which the CASP wave dataset was collected, two episodes of 16 and 18 hour duration respectively have been selected for the present analysis: from 0000 to 1500 UTC 15 February (E1), and from 2300 UTC 21 February to 1600 UTC 22 February (E2). On Fig. 2, the hourly wind speed and direction as well as the status of the three Wavec buoys are given for the two periods and for the following 10 hours. During these two periods, the three wave buoys were successfully recording hourly directional wave information, except for three hours in E2 for which some data did not pass the routine quality control test. Due to the complexity of the studied phenomenon, the selection of those two events were made to approach the ideal situation of a spatially homogeneous wind rapidly turning over an infinite fetch, in deep water, where the tendency of the local wind to align the waves in the wind direction dominates. The wind record at the two stations were compared as well as the frequency spectra of the three simultaneously recording wave buoys in order to identify cases where the wind and wave field appeared approximately homogeneous over the studied area. Offshore wind periods were eliminated to rule out any coastal effect on the wave spectrum. Also discarded were episodes of strong wind during which the low frequency local wind sea could show marked shoaling effects.

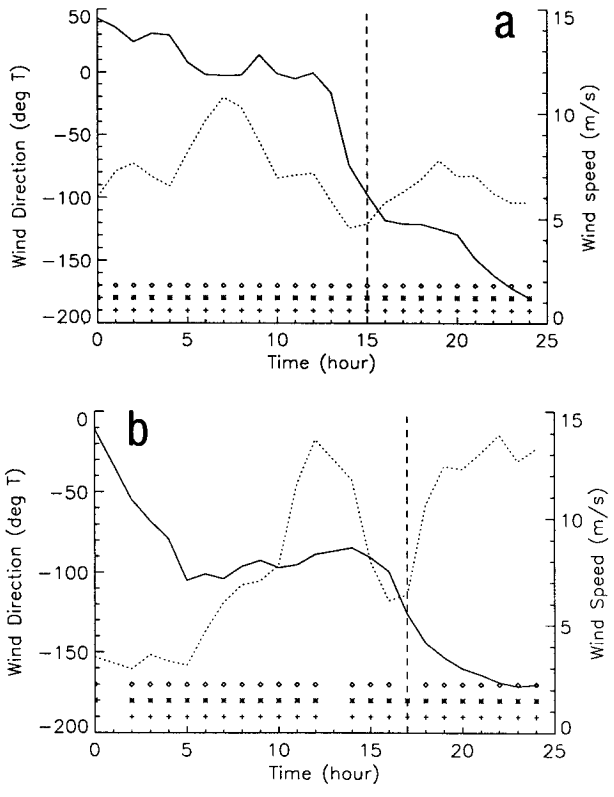


FIG. 2. Wind direction (full line) and speed (dotted line) for the two studied episodes E1 (a) and E2 (b). The wind (wave) direction is given as the direction towards which the wind (wave) is traveling. The time is given in hours from the beginning of the period. At every hour, a symbol indicates that buoy WC31 (+), WC32 (*), or WC33 (◇) was operational. A vertical dashed line indicates the end of the studied period.

For both events, the wind initially from the south gradually turns counterclockwise to become, at the end of the studied periods, parallel to the coast ($\theta_w \approx -110°$T). From that point, the wind blows offshore (slanting fetch situation), and the development of the wave field may be affected by the finite fetch. Ideally, one would like to study cases of turning wind with constant speed. However, this condition is almost never encountered in the field, and, as seen on Fig. 2, the wind during E1 and E2 significantly varies in speed as well as direction. The associated frequency sea spectra range from young partly developed to fully developed seas. Also, at all times, the wave spectrum has a strong swell component from the south, characteristic of the site as the low pressure systems generally approach from the south. The time evolution of the frequency wave spectrum at the offshore location, WC33, is given on Fig. 3 for the two studied periods and the following offshore wind episodes.

At each frequency, a mean wave direction, $\bar{\theta}(f)$, is defined in terms of the first-order moment of the spreading function:

$$\int_{\bar{\theta}(f)-\pi}^{\bar{\theta}(f)+\pi} (\theta - \bar{\theta}(f))\hat{D}(f,\theta)d\theta = 0, \qquad (7)$$

where $\hat{D}(f,\theta)$ is the IMLM estimate of the spreading function. The directional distribution is treated here as a line distribution defined on an interval of length $2\pi$ centered around a mean direction $\bar{\theta}(f)$. There might be more than one direction satisfying (7) for a given $\hat{D}(f,\theta)$. For example, a symmetric and unimodal distribution will have two possible mean directions separated by 180°. In such a situation, $\bar{\theta}(f)$ is chosen among the directions satisfying (7) as the one with maximum $\hat{D}(f,\theta)$. The use of the first-order moment (centered around the mean direction) of the directional distribution, (7), to define the mean direction elimi-

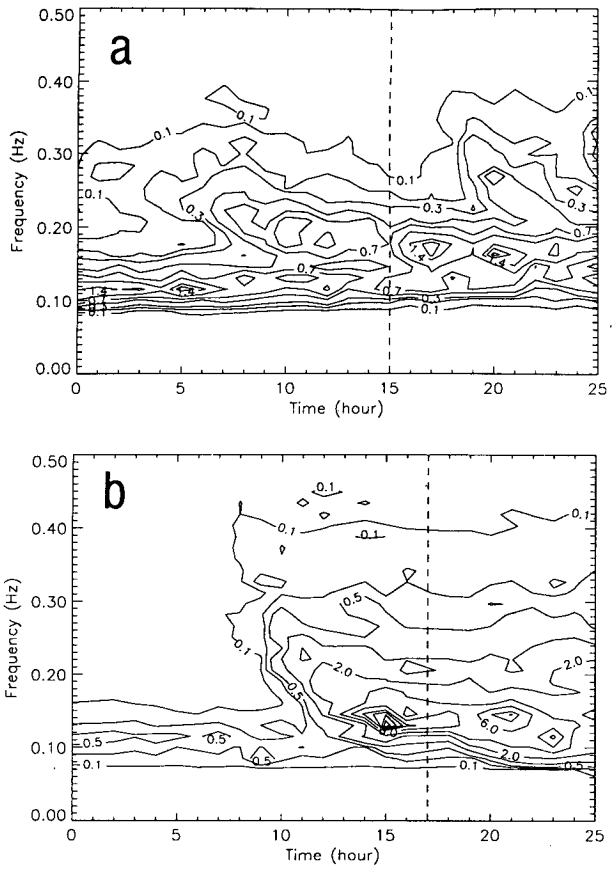


FIG. 3. Time evolution of the frequency spectra ($m^2$ $Hz^{-1}$) at WC33, for E1 (a) and E2 (b).

nates a limitation present in the two previous studies of the directional relaxation of frequency bands in which this mean direction was approximated by the phase of the first Fourier harmonic of the directional distribution. Hasselmann et al. (1980) found that the first harmonic could be predicted poorly in the case of broad, asymmetric angular distributions. For the two periods E1 and E2, an hourly $\bar{\theta}(f)$ was computed at every frequency band, for each of the three buoys. The mean direction of five frequency bands centered around 0.10, 0.20, 0.31, 0.43, and 0.54 Hz, respectively, is plotted against time in Fig. 4 (E1) and Fig. 5 (E2), along with the wind direction. As was previously observed, the wave response to the changing wind direction strongly depends on frequency, with the highest frequency band being the first to turn into the wind, and the lowest swell dominated frequency band not being affected. The mean directions for the offshore wind episodes are also given on Figs. 4 and 5. During these periods, the wave field is no longer homogeneous along the measurement array, with the response of some frequency bands at smaller fetch (WC31 and WC32) being delayed relative to the offshore location (WC33).

Following Hasselmann et al. (1980), the time rate of change of the mean wave direction at each frequency is modeled as in (2). From a one parameter regression analysis on the E1 and E2 data, the directional relaxation coefficient, $B$, was estimated for the whole interval $1.0 \leq U/c(f) \leq 2.0$ as well as for three different ranges of $U/c(f)$ within this interval. (Table 1). The time derivative in (2) was evaluated with a simple central difference scheme. In order to reduce noise from the buoy data, measurements for which the spectral density was less than one tenth of the wind sea (all frequency bands for which $U/c(f) \geq 1.0$) maximum density were discarded. Also, only deep water frequency components ($kh \geq \pi$, with $h$ the water depth) were analyzed to eliminate any finite depth effect. The resulting correlation coefficients, $0.4 \leq r \leq 0.56$, are higher than the ones obtained by Hasselmann et al. (1980) ($0.29 \leq r \leq 0.4$) and Allender et al. (1983) ($r \approx 0.25$). The average value of the relaxation coefficient, $B = 2.5 \times 10^{-5}$, is slightly higher than the estimates of these two previous studies in which they found $B = 3.1 \times 10^{-5}$ and $B = 1.7 \times 10^{-5}$, respectively. Although the present estimate of the relaxation coefficient is closer to the one obtained in Young et al. (1987) [$B \approx 4 \times 10^{-5}$ at $U/c(f) = 1.6$], there is no evidence in our data of the dependence of $B$ on the wind speed that was found in their numerical study. For the $U/c(f)$ range of the present analysis, the inclusion of the factor $U/c(f)$ in the r.h.s. of (2) does not lead to a higher correlation coefficient.

The directional relaxation process can also be examined with a different approach in which the changes in one main direction are related to the changes in the wind direction. Following Günther et al. (1981), the main wave direction of a wind-sea spectrum, $\theta_0$, is defined as the frequency integrated mean wave direction in terms of wave momentum:

$$\theta_0 = \arctan\left( \frac{\int_0^{2\pi} \int_{f_b}^{\infty} \frac{\hat{F}(f,\theta)}{c(f)} \sin\theta \, df d\theta}{\int_0^{2\pi} \int_{f_b}^{\infty} \frac{\hat{F}(f,\theta)}{c(f)} \cos\theta \, df d\theta} \right), \quad (8)$$

where

$$f_b = \begin{cases} \dfrac{0.13g}{U\cos(\theta_w - \bar{\theta}(f_b))}, & \text{if} \quad |\theta_w - \bar{\theta}(f_b)| < \dfrac{\pi}{2} \\ \infty, \quad \text{otherwise} \end{cases} \quad (9)$$

was chosen as the frequency border between the swell and the wind-sea domain, and $\hat{F}(f, \theta)/c(f)$ is the magnitude of the momentum for a spectral component of frequency $f$ and direction $\theta$. They modeled the directional relaxation of this main wave direction as

$$\frac{\partial \theta_0}{\partial t} = \chi \frac{f_b^2 U}{g} \sin(\theta_w - \theta_0) \quad (10)$$

with $g$ the gravitational acceleration, and $\chi$ the new

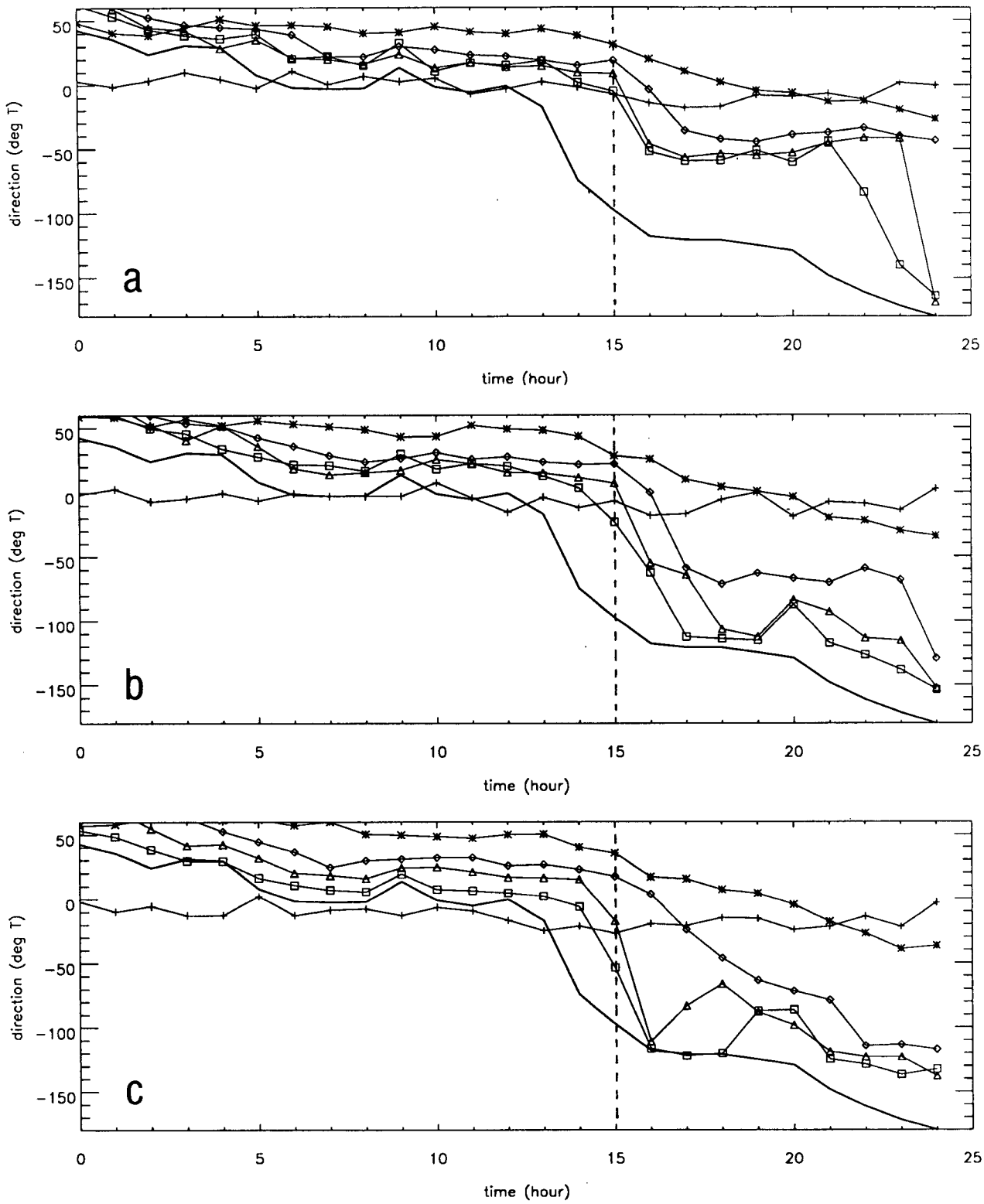


FIG. 4. Wind direction (thick line) and mean direction, for the period E1, at frequency of 0.10 (+), 0.20 (*), 0.31 (◇), 0.43 (△), and 0.54 (□) Hz, for buoy WC31 (a), WC32 (b), and WC33 (c).

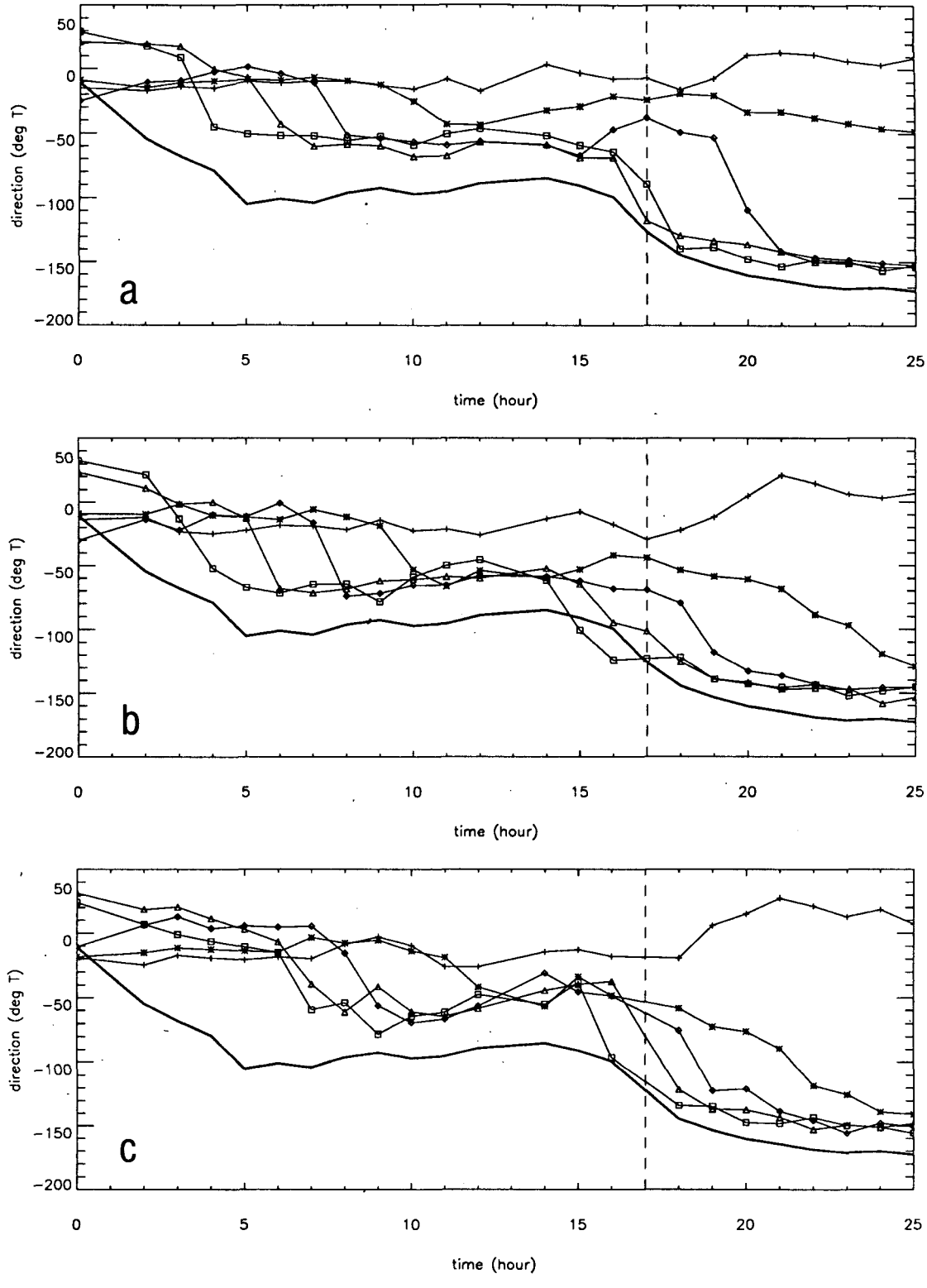


FIG. 5. As in Fig. 4 but for period E2.

TABLE 1. Results of the regression analysis of (2). The errors are standard deviations for the relaxation coefficient, $B$, and 95% confidence limits for the correlation coefficients.

| $U/c(f)$ | Entries | $B$ ($\times 10^5$) | Correlation coefficient |
|---|---|---|---|
| (1.0, 1.2) | 152 | $2.3 \pm 0.5$ | $0.40 \pm 0.14$ |
| (1.2, 1.6) | 256 | $3.8 \pm 0.4$ | $0.56 \pm 0.09$ |
| (1.6, 2.0) | 168 | $2.6 \pm 0.5$ | $0.51 \pm 0.12$ |
| (1.0, 2.0) | 576 | $3.1 \pm 0.3$ | $0.55 \pm 0.06$ |

relaxation coefficient. To obtain an estimate of $\chi$, they first identified, in four experimental cases, the lowest wave frequency to respond to the change in wind direction, and assumed that it was a good approximation for $f_b$. Four estimates of $\chi$ were then computed from (10), replacing the measured angle $(\theta_w - \theta_0)$ by the one derived from the definition of $f_b$, (9), assuming $\theta_0 \approx \bar{\theta}(f_b)$. They found an average value $\chi = 0.21 \times 10^{-2}$. In Holthuijsen et al. (1987), the relaxation of a similar main wave direction was examined which was defined as in (8) but in terms of the spectral density, $\hat{F}(f, \theta)$, instead of the momentum. Experimental cases with no swell were selected, avoiding the problem of defining a swell wind-sea boundary to evaluate the integrals in (8). Although they proposed a different relaxation model based on the growth rate of the wave energy, their eight observations of a relaxation time scale $\tau$, defined as

$$\frac{\partial \theta_0}{\partial t} = \frac{1}{\tau} \sin(\theta_w - \theta_0), \qquad (11)$$

can be used to compute the equivalent coefficient $\chi$. Using the information contained in their Table 1, an average value $\chi = 0.41 \times 10^{-2}$ was obtained from (10) and (11), in which, for these swell free cases, the border frequency, $f_b$, was simply replaced by the given peak frequency, $f_m$. In both studies, the estimated relaxation coefficient $\chi$ shows considerable scatter, ranging from $0.06 \times 10^{-2}$ up to $1.05 \times 10^{-2}$. The observations of van Vledder and Holthuijsen (1988) on the directional relaxation of the main wave direction, as defined in (8), may also be used to obtain another $\chi$ estimate. They presented results from five observations in terms of a nondimensional relaxation time scale, $\tau_* = \tau g / U_*$, and peak frequency, $\nu_* = f_m U_* / g$, with $U_*$ the friction velocity. From the given values of these two nondimensional variables an average $\chi = 0.41 \times 10^{-2}$ was computed which is in the same range as the two previous estimates. In this computation, $f_b$ in (10) was again replaced by $f_m$, and the drag coefficient used to relate $U$ and $U_*$ was defined as in van Vledder and Holthuijsen with a typical wind speed $U = 10$ m s$^{-1}$.

Using the datasets E1 and E2, a one-parameter regression analysis was performed on (10) to estimate $\chi$. However, in this analysis, the angle $(\theta_w - \theta_0)$ was taken as the measured angular difference between the wind and the main wave direction, and $f_b$ was computed according to (9). The results are presented in Table 2 (first line). The value $\chi = 0.10 \times 10^{-2}$ reported here appears to be significantly smaller than the previous estimates. This discrepancy is largely reduced when a similar regression analysis is applied to the results obtained by previous investigators. Although the average value of the combined twelve individual measurements of Holthuijsen et al. (1987) and Günther et al. (1981) is $\chi = 0.36 \times 10^{-2}$, a one parameter regression analysis done on these twelve point measurements gives a smaller $\chi = 0.17 \times 10^{-2} \pm 0.04$, which is however still larger than our $\chi$ estimate. A possible reason for this difference may be found in the choice of the studied cases. In this data, there is a relatively strong correlation ($r = 0.7$) between individual $\chi$ measurements and $|\partial\theta_0/\partial t|$, with higher values of the relaxation coefficient associated with larger time rate of change of the main wave direction. In E1 and E2, there are both periods of small and rapid change in the main wave direction, which lead to low and high values of $\chi$, respectively. There are also few cases where the main wave direction was slightly turning further away from the wind direction, resulting in small negative values for $\chi$. On the other hand, in the previous studies, only cases where there was a clearly notable change in $\theta_0$ towards the wind direction were selected, leading to larger average $\chi$ values. To further investigate this apparent discrepancy between the present $\chi$ value and the higher previous estimates, the data were reexamined by selecting cases for which the main wave direction was turning into the wind direction and the time rate of change of the main wave direction, $|\partial\theta_0/\partial t|$, was in the same range as the one used in the $\chi$ estimate of the first two previous studies

$$0.25 \times 10^{-4} \leqslant \left|\frac{\partial \theta_0}{\partial t}\right| \leqslant 1.0 \times 10^{-4} \text{ rad s}^{-1}.$$

The results are also given in Table 2 (second line). The new value $\chi = 0.12 \times 10^{-2}$ is slightly larger than the one obtained from the complete dataset, and is now within the range of values obtained by previous investigators. Although van Vledder and Holthuijsen (1988) also proposed the severity of their case selection as a possible cause for their smaller estimated time scale, the specific selection criteria used in their study (e.g., the range of $|\partial\theta_0/\partial t|$) were not given. Another possible reason that may have also contributed to the higher average $\chi$ value reported by Holthuijsen et al. (1987) is the absence of swell in the studied cases, because of possible wind-sea interactions with swell that may modify the relaxation process.

TABLE 2. Results of the regression analysis of (10). The first line gives results obtained from the whole dataset and the second line for cases with $0.25 \times 10^{-4} \leqslant |\partial\theta_0/\partial t| \leqslant 1.0 \times 10^{-4}$ rad s$^{-1}$ only. The errors are defined as for Table 1.

| $\lvert\partial\theta_0/\partial t\rvert$ | Entries | $\chi$ ($\times 10^2$) | Correlation coefficient |
|---|---|---|---|
| All | 95 | $0.10 \pm 0.01$ | $0.57 \pm 0.15$ |
| Restricted | 45 | $0.12 \pm 0.04$ | $0.51 \pm 0.24$ |

The consistency of the present estimates from the complete dataset of the two relaxation coefficients $B$ and $\chi$ can be verified by noting that the observed response of the main wave direction, $\theta_0$, is strongly dominated by the spectral components near the frequency border, $f_b$. With $\theta_0 \approx \bar{\theta}(f_b)$, we have from (2) and (10)

$$B2\pi f_b \approx \frac{\chi f_b^2 U}{g}, \tag{12}$$

or, using (9),

$$B \approx \chi \frac{0.13}{2\pi \cos(\theta_w - \theta_0)}. \tag{13}$$

With an average value $\overline{(\theta_w - \theta_0)} = -35°$, the value of the coefficient $B \approx 2.5 \times 10^{-5}$ derived from (13), with $\chi = 0.10 \times 10^{-2}$, is in very good agreement with the results of the correlation analysis. Therefore, the two time scales obtained from the discrete frequency band approach and from the integral approach are mutually consistent when both are evaluated from the complete dataset.

So far, only the lowest order moment of the directional distribution, the mean direction, has been examined. The second-order moment centered at $\bar{\theta}(f)$ can also be evaluated:

$$\sigma^2(f) = \int_{\bar{\theta}(f)-\pi}^{\bar{\theta}(f)+\pi} (\theta - \bar{\theta}(f))^2 \hat{D}(f, \theta) d\theta. \tag{14}$$

It gives the variance, or rms spread, of the directional distribution about $\bar{\theta}(f)$. In turning wind cases, the spread, $\sigma(f)$, of wind sea spectral components may be expected to be larger than in steady wind situations. For example, Kuik and Holthuijsen (1981) reported that, during a 12 hour turning wind episode, the directional width derived from a pitch-and-roll buoy increased typically 10°–15° for all observed frequencies. In Hasselmann et al. (1980), a correlation was sought between the rate of change of wind direction, $|\partial\theta_w/\partial t|$, and an approximation to $\sigma(f)$ which can be conveniently derived from the Fourier coefficients directly obtained from the buoy data. However, this approximation is strictly valid for symmetric and fairly narrow distributions only (Longuet-Higgins et al. 1963), and is known to underestimate the rms spread of broad spectra. Although they found in their data some evidence of this estimated spread increasing in turning winds, a definite correlation could not be established for the entire dataset. We performed a correlation analysis between $\sigma(f)$ and $|\partial\theta_w/\partial t|$ on the same data used to estimate the relaxation coefficients, and found a nonzero correlation throughout the whole range $1.0 \leq U/c(f) \leq 2.0$ (Table 3). The sensitivity of the spread to changes in the wind direction is greatest in the intermediate range of $U/c(f)$ where the correlation coefficient for (2) is also largest. The average spread of the measured distributions, $\sigma = 45°$, is slightly larger than the one expected for waves generated by a constant wind vector, $\sigma = 38.8°$. The latter spread value is obtained by averaging the rms spread [as defined in (14)] of the standard Mitsuyasu–Hasselmann form of the spreading function (cf. Hasselmann et al. 1980) over the appropriate range $1.0 \leq U/c(f) \leq 2.0$.

TABLE 3. Results of the regression analysis between the directional spread, $\sigma$, and the rate of change of the wind, $|\partial\theta_w/\partial t|$. The errors are defined as for Table 1.

| $U/c(f)$ | Entries | $\bar{\sigma}$ (deg) | Correlation coefficient |
|---|---|---|---|
| (1.0, 1.2) | 152 | 43 ± 11 | 0.32 ± 0.15 |
| (1.2, 1.6) | 256 | 45 ± 12 | 0.46 ± 0.11 |
| (1.6, 2.0) | 168 | 46 ± 10 | 0.30 ± 0.14 |
| (1.0, 2.0) | 576 | 45 ± 11 | 0.36 ± 0.07 |

A final analysis has been done to look at the shapes of the directional distributions in terms of unimodality and symmetry about the mean direction. Obviously, the simple relaxation models reported in this paper cannot properly represent the complex response of multimodal distributions to turning winds. This may be a cause for the large scatter of the relaxation coefficients measured by different authors, and also for the large standard deviations for the coefficients reported in Tables 1 and 2. In the numerical study of Young et al. (1987), the results showed bimodal distributions for wind shifts larger than 60°. It would be interesting to test field data for this behavior. Unfortunately, pitch-and-roll buoy data are not well suited to detect bimodality. Although the high precision of the IMLM estimates has been demonstrated for many different test spectra, they also show occasional inaccuracy. In particular, the method has been demonstrated to improperly resolve bimodal distributions when the peaks are too close to each other (e.g., Oltman-Shay and Guza 1984). In such a situation, a single peak is placed between the true peaks, skewed towards the more energetic mode. Although the IMLM is not expected to resolve all bimodal distributions present in the data, a simple test was applied on the estimated directional distributions to identify distributions that were (nearly) unimodal and symmetric (as in Kuik et al. 1988, their Appendix 2). All the directional distributions used in the correlation analyses were tested, and a proportion of 39% and 17% of the distributions were found clearly not symmetric and not unimodal for the periods E1 and E2, respectively. For example, on Fig. 6, the time evolution of the spectrum, $\hat{F}(f, \theta)$, is given for an intermediate frequency band centered around $f = 0.25$ Hz, during E1. At the beginning of the period, the estimated distribution shows a well defined bimodal structure, with one peak near the swell direction, and the second peak near the actual wind direction. This was a common behaviour for intermediate frequency bands during this period. These results indicate that a significant portion of the present data exhibits neither symmetric nor unimodal distributions for frequency components responding to the wind, with evidence of bimodal structure as predicted by numerical experi-

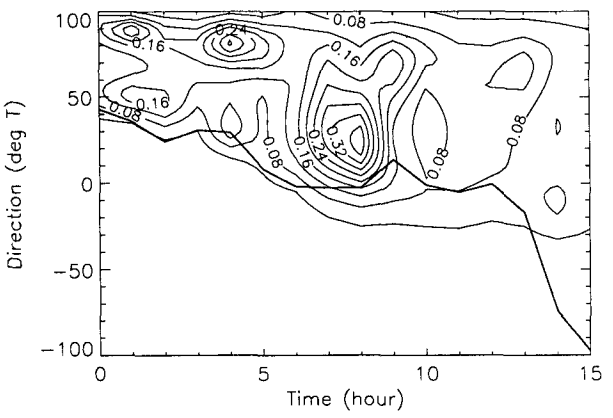


FIG. 6. Time evolution of the directional spectrum, $\hat{F}(f, \theta)$, ($m^2$ $Hz^{-1}$) at frequency $f = 0.25$ Hz, and the wind direction (thick line), for the period E1.

ments. This points out the inadequacy of the simple relaxation models to account for all aspects of the complex relaxation process.

## 4. Summary

Directional wave spectra were estimated from data collected by an array of three Wavec buoys during CASP 86. The iterative maximum likelihood method (IMLM) was used to obtain high resolution estimates of the wave directional distributions. Two turning wind events were selected for which the response of the waves to the changing wind direction was analyzed. The relaxation coefficient for the mean direction of individual frequency bands, first introduced by Hasselmann et al. (1980), was estimated for the range $1.0 \leqslant U/c(f) \leqslant 2.0$, with an average value $B = 3.1 \times 10^{-5}$. The response of one main wave direction for the whole wind-sea spectrum, as defined to Günther et al. (1981), was also studied, with a resulting average relaxation coefficient $\chi = 0.10 \times 10^{-2}$. Although this $\chi$ value is significantly smaller than the estimates obtained in previous studies, it is found to be consistent with the present estimate of the coefficient $B$, assuming the response of $\chi$ to be dominated by frequencies near the swell wind-sea boundary. The apparent discrepancy between the previous estimates of the two classes of relaxation time scales is explained here by the differences in the methods of analysis and by the selection of the studied cases. In fact, when only cases for which the time rate of change of the main wave direction is in the range studied by Günther et al. (1981) and Holthuijsen et al. (1987) are considered, and when a similar one parameter regression analysis is applied to their data, the relaxation coefficient $\chi = 0.22 \times 10^{-2}$ is now within the range of their results.

The wave rms directional spread about the mean direction was also derived from the computed distributions. A definite correlation was established for the first time between the directional spread of the waves and the rate of change of wind direction. Finally, although the IMLM may not properly resolve all bimodal distributions, the shape of the spreading functions were tested for unimodality and symmetry about the mean direction. In the two studied periods, 39% and 17%, respectively, of the distributions were neither unimodal nor symmetric, with clearly bimodal distributions for some intermediate frequency bands adjusting to the changing wind direction.

*Acknowledgments.* Thanks are expressed to the CASP 86 participants for the opportunity to use the data collected during this experiment, and especially to Bechara Toulany for kindly providing us with the data. We also thank Wing Quan for assistance in processing the data.

## REFERENCES

Allender, J. H., J. Albrecht and G. Hamilton, 1983: Observations of directional relaxation of wind sea spectra. *J. Phys. Oceanogr.*, **13,** 1519–1525.

Dobson, F., W. Perrie and B. Toulany, 1989: On the deep-water fetch laws for wind-generated surface gravity waves. *Atmos. Ocean,* **27**(1), 210–236.

Donelan, M. A., J. Hamilton and W. H. Hui, 1985: Directional spectra of wind-generated waves. *Phil. Trans. Roy. Soc. London,* **A315,** 509–562.

Günther, H., W. Rosenthal and M. Dunckel, 1981: The response of surface gravity waves to changing wind direction. *J. Phys. Oceanogr.*, **11,** 718–728.

Hasselmann, D. E., M. Dunckel and J. A. Ewing, 1980: Directional wave spectra observed during JONSWAP 1973. *J. Phys. Oceanogr.*, **10,** 1264–1280.

Holthuijsen, L. H., A. J. Kuik and E. Mosselman, 1987: The response of wave directions to changing wind directions. *J. Phys. Oceanogr.*, **17,** 845–853.

Krogstad, H. E., R. L. Gordon and M. C. Miller, 1988: High-resolution directional wave spectra from horizontally mounted acoustic Doppler current meters. *J. Atmos. Oceanic. Technol.*, **5,** 340–352.

Kuik, A. J., and L. H. Holthuijsen, 1981: Buoy observations of directional wave parameters. *Proc. Conf. on Directional Wave Spectra Applications.* New York, R. L. Wiegel, Ed., University of California, Berkeley, ASCE, 61–70.

——, G. Ph. van Vledder and L. H. Holthuijsen, 1988: A method for the routine analysis of pitch-and-roll buoy wave data. *J. Phys. Oceanogr.*, **18,** 1020–1034.

Longuet-Higgins, M. S., D. E. Cartwright and N. D. Smith, 1963: Observations of the directional spectrum of sea waves using the motions of a floating buoy. *Ocean Wave Spectra,* Prentice Hall, 111–136.

Mitsuyasu, H., F. Tasai, T. Suhara, S. Mizuno, M. Ohkusu, T. Honda and K. Rikiishi, 1975: Observations of the directional spectrum of ocean waves using a cloverleaf buoy. *J. Phys. Oceanogr.*, **5,** 750–760.

Oltman-Shay, J., and R. T. Guza, 1984: A data-adaptive ocean wave directional-spectrum estimator for pitch and roll type measurements. *J. Phys. Oceanogr.*, **14,** 1800–1810.

Pawka, S. S., 1983: Island shadows in wave directional spectra. *J. Geophys. Res.*, **88**(C4), 2579–2591.

van Vledder, G. Ph., and L. H. Holthuijsen, 1988: Waves in turning windfields. *Proc. 21st Coastal Engineering Conf.,* Malaga, ASCE, 602–611.

Young, I. R., S. Hasselmann and K. Hasselmann, 1987: Computations of the response of a wave spectrum to a sudden change in wind direction. *J. Phys. Oceanogr.*, **17,** 1317–1338.